Chinese Chemical Letters 32 (2021) 2792–2796

Contents lists available at ScienceDirect

Chinese Chemical Letters

journal homepage: www.elsevier.com/locate/cclet

Communication

Sequential separation of Cu(II)/Ni(II)/Fe(II) from strong-acidic pickling wastewater with a two-stage process based on a bi-pyridine chelating resin

Yingzhi Lv[a], Lidan Zong[a], Zicheng Liu[a], Jianwei Du[c], Fenghe Wang[d], Yanhong Zhang[a,e], Chen Ling[b,*], Fuqiang Liu[a,*]

[a] State Key Laboratory of Pollution Control and Resource Reuse, School of the Environment, Nanjing University, Nanjing 210023, China
[b] College of Biology and the Environment, Nanjing Forestry University, Nanjing 210037, China
[c] South China Institute of Environmental Sciences, Ministry of Ecology and Environment, Guangzhou 510530, China
[d] Jiangsu Key Laboratory of Material Cycle and Pollution Control, School of Environment, Nanjing Normal University, Nanjing 210023, China
[e] Jiangsu Provincial Key Laboratory of Environmental Engineering, Jiangsu Provincial Academy of Environmental Science, Nanjing 210036, China

ARTICLE INFO

Article history:
Received 23 October 2020
Received in revised form 12 December 2020
Accepted 19 January 2021
Available online 27 January 2021

Keywords:
Bi-pyridine chelating resin
Separation
Dense Fe(II)
Strong-acidity
Pickling wastewater

ABSTRACT

A self-synthesized bi-pyridine chelating resin (PAPY) could separate Cu(II)/Ni(II)/Fe(II) sequentially from strong-acidic pickling wastewater by a two-stage pH-adjusted process, in which Cu(II), Ni(II), and Fe(II) were successively preferred by PAPY. In the first stage (pH 1.0), the separation factor of Cu(II) over Ni(II) reached 61.43 in Cu(II)-Ni(II)-Fe(II) systems. In the second stage (pH 2.0), the separation factor of Ni(II) over Fe(II) reached 92.82 in Ni(II)-Fe(II) systems. Emphasis was placed on the selective separation of Cu(II) and Ni(II) in the first-stage. The adsorption amounts of Cu(II) onto PAPY were 1.2 mmol/g in the first stage, while those of Ni(II) and Fe(II) were lower than 0.3 mmol/g. Cu(II) adsorption was hardly affected by Ni(II) with the presence of dense Fe(II), but Cu(II) inhibited Ni(II) adsorption strongly. Part of preloaded Ni(II) could be replaced by Cu(II) based on the replacement effect. Compared with the absence of Fe(II), dense Fe(II) could obviously enhance the separation of Cu(II)-Ni(II). More than 95.0% of Cu(II) could be removed in the former 240 BV (BV for bed volume of the adsorbent) in the fixed-bed adsorption column process with the flow rate of 2.5 BV/h. As proved by X-ray photoelectron spectrometry (XPS) and density functional theory (DFT) analyses, Cu(II) exerted a much stronger deprotonation and chelation ability toward PAPY than Ni(II) and Fe(II). Thus, the work shows a great potential in the separation and purification of heavy metal resources from strong-acidic pickling wastewaters.

Pickling wastewater commonly occurs during the descaling and polishing of steel and other basic metal pieces which contains rich heavy metal ions (HMIs, including Cu(II), Ni(II), dense Fe(II), *etc.*) [1,2]. This kind of waste water is highly acidic (pH 1.0–3.0) and can bring serious environmental disasters before effective treatment [3,4]. Many big steel plants around the world applied the process of neutralization-precipitation, which led to harmful sludges and waste of resources [5]. Recently, the recycling treatment of metals and acids in pickling wastewater has become a hot topic. The selective pre-removal of the coexisting HMIs in pickling wastewater is very important but often overlooked during the resource/water reclamation such as recovering Fe(II) to prepare flocculants [6,7]. Thus, separating and recycling HMIs, as scarce resources, are of much significance in environment and economy [8–10].

Liquid-liquid extraction and solid-phase extraction (including ion exchange and chelating adsorption) are common methods in purification and separation of HMIs [11–13]. However, the efficiency mostly decreased significantly at lower pH, which limited their application in dealing with the strong-acidic pickling wastewater [14–17].

Such commercial resins containing bi-pyridine groups as M4195 and TP220 were reported earlier to be effective even at pH 1.0 [18,19]. The preferred HMIs were in the order of Cu(II) > Ni(II) > Co(II) [20,21]. The feature is attributed to (1) low p*K*a value of pyridine N and (2) complexes with stable configuration formed between HMIs and pyridine. In our previous work, a novel chelating resin bearing more imino-bi-pyridine groups (PAPY) was self-synthesized with a relative green and economical route, which

* Corresponding authors.
E-mail addresses: leeche90109@126.com (C. Ling), lfq@nju.edu.cn (F. Liu).

https://doi.org/10.1016/j.cclet.2021.01.038

exhibited much higher adsorption capacity and selectivity to Ni(II) over Co(II) compared with M4195 and TP220 at a wide pH range ($\geq$ 2.0) [22]. However, little is known about the application feasibility of PAPY in HMIs separation from strong-acidic pickling wastewater containing dense Fe(II). Due to its excellent acid-resistant ability and distinct chelating affinities to different HMIs, PAPY is expected to separate concurrent HMIs sequentially from pickling wastewater containing dense Fe(II).

Thus, this work aimed to investigate the separation properties of Cu(II), Ni(II) and Fe(II) by the self-synthesized bi-pyridine resin (PAPY, the synthesis route was detailed in Supporting information) and develop a pH-adjusted two-stage process to separate the HMIs sequentially and efficiently. The separation behaviors and mechanisms of Cu(II) and Ni(II) from strong-acidic and high-ferrous pickling wastewater in the first-stage separation were highlighted with static and kinetic experiments, X-ray photoelectron spectrometry (XPS) characterization and density functional theory (DFT) calculations.

As shown in Fig. S1 (Supporting information), the appropriate pH range for the sole-solute adsorption of Cu(II)/Ni(II)/Fe(II) by PAPY was obviously different, which created the possibility of their effective separation by adjusting the solution pH. The highly selective and efficient removal of Cu(II) from Cu(II)-Ni(II)-Fe(II) tri-solute system, and Ni(II) from Ni(II)-Fe(II) bi-solute system were indeed achieved at pH 1.0 and 2.0, respectively (Fig. 1). At pH 1.0, Cu(II) maintained to be highly adsorbed in all mixed-solute systems even when the concentration of Fe(II) was 10 mmol/L. Meanwhile, the adsorption capacity of Ni(II) was inhibited by Cu(II) to a great extent. On the other hand, at pH 2.0, Ni(II) could be further separated from Fe(II) with the high adsorption amount ($Q_{e,\ Ni(II)}$ = 0.94 mmol/g) and the better selectivity (α_{Fe}^{Ni}) in Ni(II)-Fe(II) bi-solute system without Cu(II). Thus, the trends well suggested that the sequential separation of Cu(II)/Ni(II)/Fe(II) could be achieved by adjusting pH value (Fig. S2 in Supporting information). Moreover, PAPY exhibited superior selective performance for Cu(II) compared with other four commercial chelating resins (whose main structures and features were listed in Table S1 in Supporting information), including two bi-pyridine resins (M4195 and TP220), iminodiacetic resin (IRC748) and amidophosphoric acid resin (S950). Their separation properties and selective parameters were shown in Fig. S3 (Supporting information). Because HMIs were preferred following the order as Cu(II), Ni(II), Fe(II) successively, preferential separation of Cu(II) from Cu(II)-Ni(II)-Fe(II) tri-solute system is the prerequisite and important for sequential separation. Therefore, the following parts would mainly focus on exploring the separation properties and mechanisms of Cu(II) and Ni(II) from strong-acidic and high-ferrous pickling wastewater by PAPY at pH 1.0.

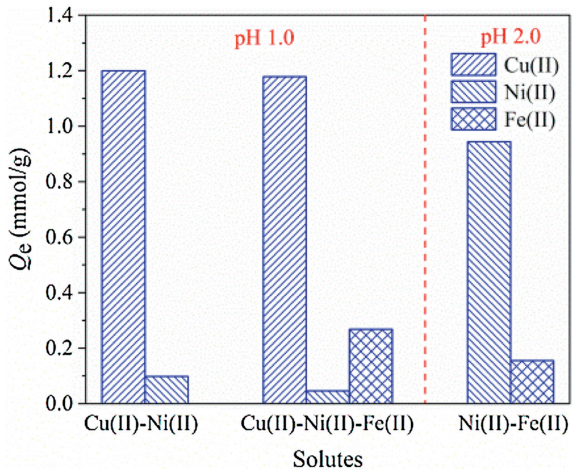

Fig. 1. Adsorption capacity of PAPY in mixed solutions under different conditions (resin dosage = 0.5 g/L; V = 50 mL; t = 24 h; T = 298 K; $C_{0,\ Cu(II)}$ = 1 mmol/L, $C_{0,\ Ni(II)}$ = 1 mmol/L, $C_{0,\ Fe(II)}$ = 10 mmol/L; pH 1.0 in Cu(II)-Ni(II) and Cu(II)-Ni(II)-Fe(II) systems, pH 2.0 in Ni(II)-Fe(II) system).

The equilibrium isotherms of Cu(II)/Ni(II) were investigated in Cu(II)-Ni(II)-Fe(II) tri-solute system. The three-dimensional isotherm images with the concentration of Cu(II) and Ni(II) as the factors were fitted with extended Langmuir model (ELM) and modified Langmuir model (MLM) (Fig. S4 in Supporting information). The fitted parameters were shown in Table 1. Cu(II)/Ni(II) adsorption amounts increased with its equilibrium concentration at a fixed Cu(II)/Ni(II) concentration until all the available sites were consumed. Cu(II) adsorption was hardly affected by Ni(II) while Ni(II) uptake was much suppressed with the increase of $C_{e,\ Cu(II)}$ and showed a concave shape. $Q_{e,\ Cu(II)}$ decreased by 5.72%–1.51% with the highest $C_{0,\ Ni(II)}$ at $C_{0,\ Cu(II)}$ from 0.5 mmol/L to 4 mmol/L. Correspondingly, $Q_{e,\ Ni(II)}$ decreased by 36.63%–51.22% with the highest $C_{0,\ Cu(II)}$ at $C_{0,\ Ni(II)}$ from 0.5 mmol/L to 4 mmol/L. The adsorption data could be better fitted by ELM with a relative lower RSS value (<<1). K_{ELM} reflects the binding affinity between adsorbent and adsorbate while η represents the instability of HMIs adsorption affected by the other HMIs. Therefore, the much higher $K_{ELM,\ Cu(II)}$ and much lower η_{Cu} than those of Ni(II) both confirmed that Cu(II) was the preferred species for binding with PAPY, and to some degree, the binding affinity to Cu(II) was 94.7 times higher than Ni(II). The separation factors of Cu(II) over Ni(II) at different molar ratios were tabulated in Table S2 (Supporting information). The α_{Ni}^{Cu} values ranged from 10.98 to 140.64 with the increased Ni(II) concentration and the decreased Cu(II) concentration. All the results indicated that Cu(II) could be highly selective removed by PAPY while Ni(II) was retained in the aqueous system containing dense Fe(II) and H^+.

The kinetic adsorption of Cu(II)/Ni(II) in Cu(II)-Ni(II) bi-solute system and Cu(II)-Ni(II)-Fe(II) tri-solute system were shown in Fig. 2. The adsorption capacity of Cu(II) increased with time while that of Ni(II) rose at the initial stage but then reduced in both systems. The decreased uptake of Ni(II) was probably resulted from the replacement of Cu(II) for its higher binding affinity with PAPY. Moreover, it was noteworthy that Ni(II) adsorption reached the maximum far earlier (40 min) than that without Fe(II) (about 810 min). Besides, the equilibrium adsorption amount of Ni(II) obviously decreased by 38.2% with the presence of Fe(II). In contrast, both adsorption amount and adsorption rate of Cu(II) were hardly impacted by Fe(II) which can be proved by the superposed curves and approximate parameter values in PFOM and PSOM (Table S3 in Supporting information). It means that Fe(II) could enhance the separation performance of Cu(II) and Ni(II) considering both the increased separation factor and replacement rate.

The separation properties were further evaluated in a fixed-bed dynamic experiment for simulating the practical operation. The breakthrough curves of Cu(II)/Ni(II) were shown in Fig. 3. The breakthrough point volume (BPV, set as C_t/C_0 = 0.05) and the saturation point volume (SPV, set as C_t/C_0 = 0.90) were all listed in

Table 1
Fitting parameters of three-dimensional isotherm models from Cu(II)-Ni(II)-Fe(II) system.

Isotherm models	Extended Langmuir model	Modified Langmuir model
Parameters	RSS = 0.0229 Q_{max} =1.31 mmol/g $K_{ELM,\ Cu(II)}$ = 7.3714 $K_{ELM,\ Ni(II)}$ = 0.0778	RSS = 0.1191 $\eta_{Cu(II)}$ = 1.2287 $\eta_{Ni(II)}$ = 13.6426

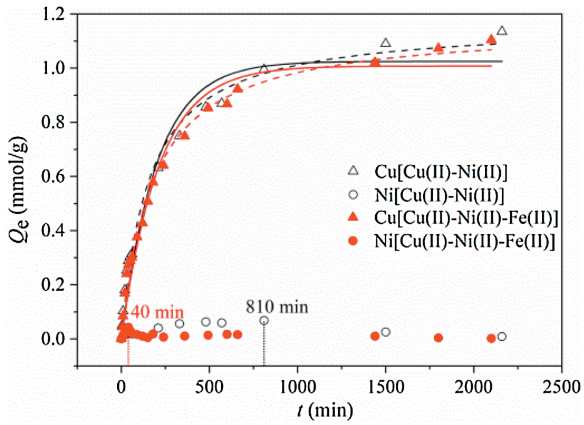

Fig. 2. Adsorption kinetic studies of Cu(II)/Ni(II) in mixed solutions onto PAPY fitted by *pseudo*-first-order (solid lines) and *pseudo*-second-order (dashed lines) models (resin dosage = 0.5 g/L; V = 50 mL; T = 298 K; $C_{0,\,Cu(II)}$ = 1 mmol/L, $C_{0,\,Ni(II)}$ = 1 mmol/L, $C_{0,\,Fe(II)}$ = 10 mmol/L; pH 1.0).

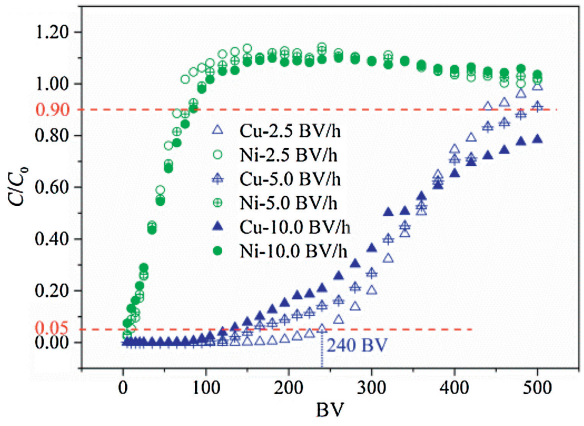

Fig. 3. Breakthrough curves for simultaneous adsorption of Cu(II)/Ni(II) onto PAPY in Cu(II)-Ni(II)-Fe(II) system (resin dosage = 0.5 g/L; V = 50 mL; T = 298 K; $C_{0,\,Cu(II)}$ = 1 mmol/L, $C_{0,\,Ni(II)}$ = 1 mmol/L, $C_{0,\,Fe(II)}$ = 10 mmol/L; pH 1.0).

Table S4 (Supporting information). More than 95.0% of Cu(II) could be removed in the former 240 BV (BV for bed volume of the adsorbent) at the flow rate of 2.5 BV/h. The BPV of Cu(II) obviously increased with the decreased flow rate while that of Ni(II) was almost unchanged. The trend was resulted from the more sufficient interaction between solutes and resins. Unexpectedly, the effluent concentrations of Ni(II) at the later period had exceeded its influent ones, which again reflected the replacement effect of Cu(II) on Ni(II) [23]. The replacement seemed to be strengthened at a lower flow rate for more adequate contact time.

XPS and DFT analyses were conducted to reveal the mechanisms behind the highly efficient separation of Cu(II) and Ni(II) by PAPY in the presence of dense Fe(II) and H^+. The XPS wide scans and N 1s high-resolution spectra of PAPY before and after metal ions adsorption with concentration of 1.0 mmol/L at pH 1.0 were compared in Fig. 4. The XPS high resolution spectra of Cu 2p, Ni 2p and Fe 2p indicated that complexation exists between the PAPY chelating groups and heavy metal ions (Fig. S5 in Supporting information). The N 1s spectra of fresh PAPY was disassembled into three branch peaks at around 398.11 eV (N1), 399.46 eV (N2), 398.73 eV (N3), pointing to the neutral amine (-NH or C-N), protonated amine (-NH_2^+ or -NH^+), pyridine moiety (C=N), respectively [24–27]. Comparing with PAPY treated with acidic water at pH 1.0, the binding energy (BE) of N1 and N3 shifted to the higher BE by 0.53−0.70 eV after the capture of sole Cu(II), 0.47−0.68 eV for the case of Ni(II) and 0.34−0.42 eV for the case of Fe(II), respectively. The changes suggested both neutral amine-N and pyridine-N donated the long pair of electrons to form a coordination bond with the metals, with the extent in the order of Cu(II) > Ni(II) > Fe(II) at the tested condition [28,29]. More importantly, the N2 area all decreased after HMIs adsorption, indicating that the secondary amino group was unprotonated in different degree. The N2 area in the sample of PAPY-Cu and PAPY-Ni were dropped by 18.3% and 11.2%, respectively, while that for PAPY-Fe only reduced by 7.3%. The difference suggested that the majority of H^+ attracted aside N atom could be more easily squeezed out by Cu(II) than Ni(II)/Fe(II). It was probably attributed to the higher electronegativity of Cu(II) and stronger binding affinity between Cu(II) and PAPY at pH 1.0, which would be further proved by DFT.

As mentioned above, the interaction affinity of PAPY toward metal ions and the deprotonation abilities of PAPY by HMIs were in the same order of Cu(II) > Ni(II) > Fe(II). It was well consistent with the reported articles [30,31]. As the radius of metal ion decreased, the electronegativity of metal ion increased and the stability of the complex increased. Theoretically, as shown in Fig. 5, there were three kinds of N atoms in one-unit structure of PAPY, all of which could contribute to the chelating adsorption of HMIs. Under acidic conditions, N in amines and pyridines tended to attract H^+ from aqueous phase and could also be deprotonated when the pH was higher than its pKa. The pKa values of them in the sulfate solutions (N①:1.5, N②:2.7, N③:3.5) revealed that they were almost all protonated at pH 1.0. Thus, Cu(II) could replace all the three H^+ while Ni(II) and Fe(II) might only replace the H^+ in protonated pyridine nitrogen due to their difference in deprotonation ability.

Therefore, complex structures of three HMIs were proposed in Fig. S6 (Supporting information) and evaluated from energy view by DFT optimization. The main structure parameters were listed in Table S5 (Supporting information). The PAPY-Cu complex, was a tridentate ligand with two five-member ring structure, while PAPY-Ni and PAPY-Fe complex were bidentate ligands with eight-member ring structure. The absolute value of binding energy (ΔE) of PAPY-Cu complex was 809.5 kJ/mol and 1028.7 kJ/mol higher than that of PAPY-Ni and PAPY-Fe complex, respectively. Thus, PAPY had high affinity to Cu(II) and was hard to be interfered by Ni(II) and Fe(II).

Furthermore, the separation mechanisms of PAPY could be illuminated with two steps including deprotonation and chelation illustrating in Fig. 5. In Step I, HMIs replaced the H^+ to contend for lone pair electrons of nitrogen atoms. In Step II, the deprotonated nitrogen atoms regained the ability to coordinate with HMIs. However, the advantage component Cu(II) owned the strongest affinity and thus could be preferentially adsorbed onto PAPY. Moreover, the presence of dense Fe(II) prevented Ni(II) from approaching the site of PAPY, which led to the effective replacement of Ni(II) (the inferior species) by Cu(II) (the favorable species).

A real pickling wastewater experiment was conducted to test the practical application ability of PAPY. The result suggests that PAPY has characteristic and feasibility in separating Cu(II) selectively from real pickling wastewater (Table S6 in Supporting information).

In this work, the sequential separation of Cu(II)/Ni(II)/Fe(II) was achieved through a two-stage adsorption process in which pH was orderly adjusted to 1.0 and 2.0. In the first-stage (pH 1.0) separation of Cu(II) and Ni(II) from dense Fe(II) and H^+, PAPY exhibited not only the higher Cu(II) adsorption amount ($Q_{e,\,Cu(II)}$ = 1.2 mmol/g) but also the higher separation factor (α_{Ni}^{Cu} = 61.43) compared with four commercial resins. The presence of dense Fe(II) could enhance

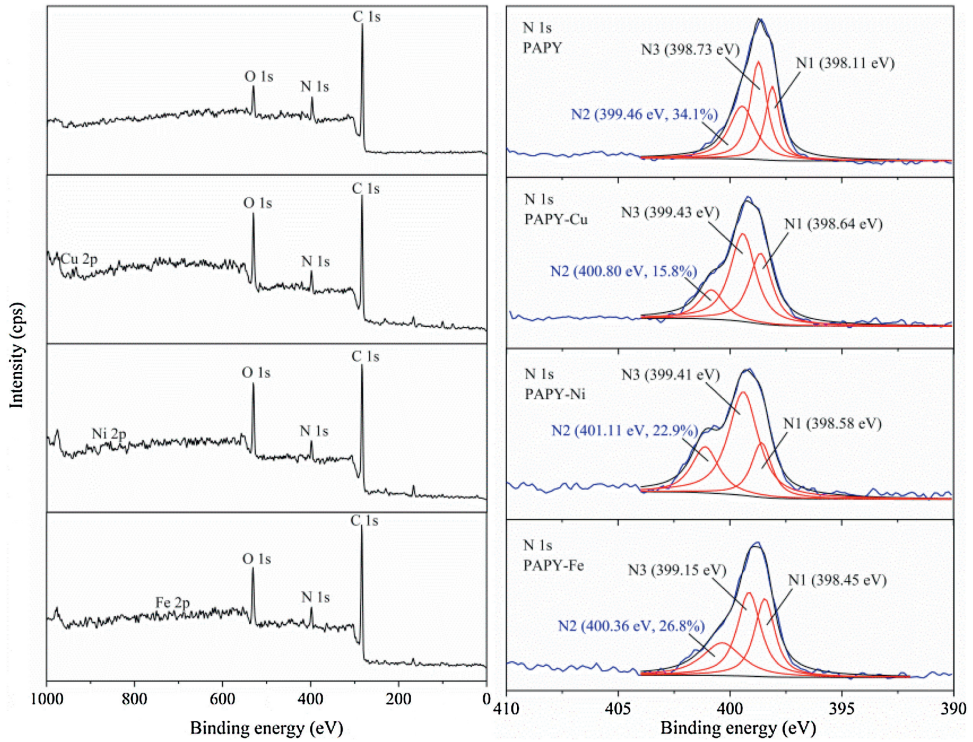

Fig. 4. (a) XPS wide scans and (b) N 1s spectra of PAPY before and after loading with Cu(II)/Ni(II)/Fe(II) (N1 for -NH or C-N, N2 for $-NH_2^+$ or $-NH^+$, N3 for pyridine nitrogen C=N).

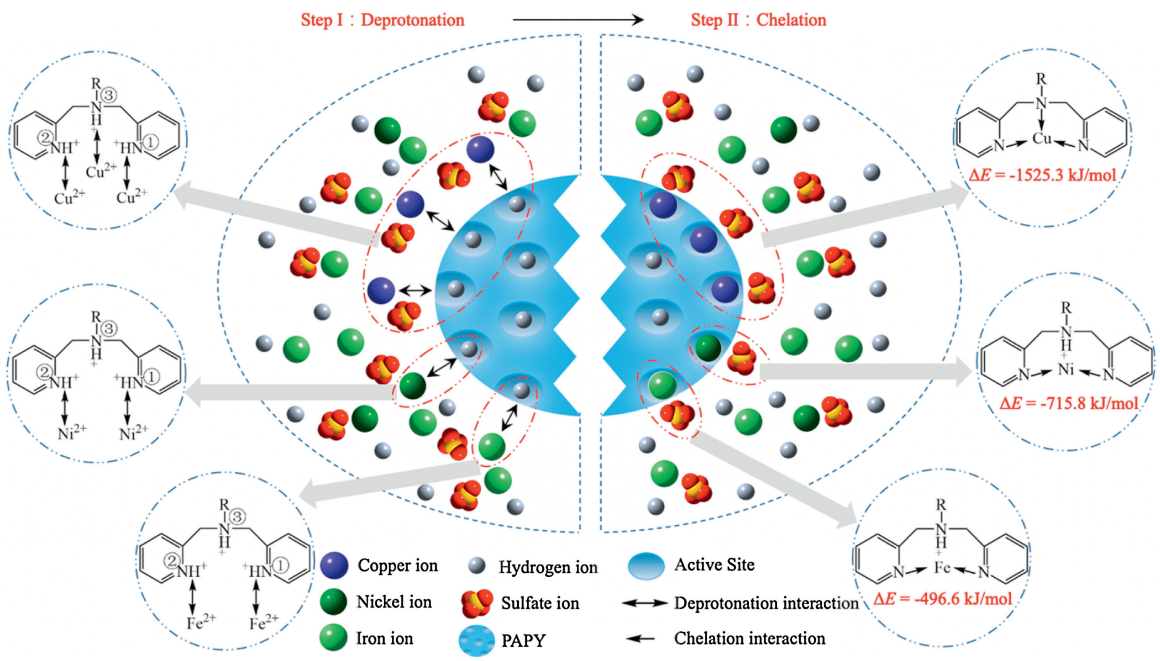

Fig. 5. Schematic diagram of the separation mechanisms for Cu(II) and Ni(II) onto PAPY from high-concentration ferrous solution.

the separation of Cu(II) and Ni(II) as the adsorption amount and adsorption rate of Cu(II) almost kept constant while those of Ni(II) decreased. The dynamic results revealed that the removal efficiency of Cu(II) was more than 95.0% in the former 240 BV at the flow rate of 2.5 BV/h. XPS and DFT analyses proved that the main mechanisms included deprotonation and chelation processes. In summary, PAPY possesses the high potential in separating and recovering HMIs sequentially from the pickling wastewater.

Declaration of competing interest

The authors declare that they have no known competing financial interests or personal relationships that could have appeared to influence the work reported in this paper.

Acknowledgments

This work was supported by the National Natural Science Foundation of China (Nos. 51878334, 51522805) and the Natural Science Foundation of Jiangsu Province, China (No. BK20170647).

Appendix A. Supplementary data

Supplementary material related to this article can be found, in the online version, at doi:https://doi.org/10.1016/j.cclet.2021.01.038.

References

[1] M.T. Wu, Y.L. Li, Q. Guo, et al., J. Clean. Prod. 240 (2019) 1–7.
[2] X.Y. Zhan, L.A. Wang, L. Wang, et al., Colloid Surf. A: Physicochem. Eng. Asp. 577 (2019) 523–531.
[3] S. Yang, W. Li, H. Zhang, Y. Wen, Y. Ni, Sep. Purif. Technol. 209 (2019) 238–245.
[4] A. Devi, A. Singhal, R. Gupta, P. Panzade, Clean Technol. Environ. Policy 16 (2014) 1515–1527.
[5] M.S. Yeh, H.H. Ou, Y.C. Su, P.H. Lin, J. Environ. Eng. 142 (2016) 05016003.
[6] Y. Li, X. Tian, X. He, et al., Environ. Sci. Pollut. Res. 27 (2020) 37011–37021.
[7] D.T. Nguyen, L.T. Pham, H.T.T. Le, et al., RSC Adv. 8 (2018) 19707–19712.
[8] Y. Liu, W. Zhang, C. Zhao, et al., Chem. Eng. J. 361 (2019) 528–537.
[9] Z. Dong, J.Z. Liu, W.J. Yuan, Y.P. Yi, L. Zhao, Chem. Eng. J. 283 (2016) 504–513.
[10] J.H. Ma, Y.T. Liu, O. Ali, et al., J. Hazard. Mater. 344 (2018) 1034–1042.
[11] Y. Zhu, Z.S. Bai, H.L. Wang, Chin. Chem. Lett. 28 (2017) 633–641.
[12] Y. Chang, C. Shen, P.Y. Li, et al., Chin. Chem. Lett. 28 (2017) 319–323.
[13] F. Hu, H.P. Hu, J.P. Yang, et al., J. Mol. Liq. 291 (2019) 8.
[14] G.X. Zhao, X.B. Huang, Z.W. Tang, et al., Polym. Chem. 9 (2018) 3562–3582.
[15] Q. Chen, J.W. Zheng, L.C. Zheng, Z. Dang, L.J. Zhang, Chem. Eng. J. 350 (2018) 1000–1009.
[16] S. Radi, C. El Abiad, N.M.M. Moura, Z. Dang, L.J. Zhang, J. Hazard. Mater. 370 (2019) 80–90.
[17] J. Ma, J. Shen, C. Wang, Y. Wei, J. Taiwan, Inst. Chem. Eng. 91 (2018) 532–538.
[18] D. Kolodynska, W. Sofinska-Chmiel, E. Mendyk, Y. Wei, Sep. Sci. Technol. 49 (2014) 2003–2015.
[19] M.D. Ogden, E.M. Moon, A. Wilson, S.E. Pepper, Chem. Eng. J. 317 (2017) 80–89.
[20] P. Littlejohn, J. Vaughan, Hydrometallurgy 121 (2012) 90–99.
[21] A. Wolowicz, Z. Hubicki, Chem. Eng. J. 197 (2012) 493–508.
[22] L. Zong, F. Liu, D. Chen, et al., Chem. Eng. J. 334 (2018) 995–1005.
[23] S. Dang, L. Zhao, Q. Yang, et al., Chem. Eng. J. 328 (2017) 172–185.
[24] I. Bertoti, M. Mohai, K. Laszlo, Carbon 84 (2015) 185–196.
[25] Z. Zhu, M. Zhang, W. Wang, Q. Zhou, F. Liu, Sci. Rep. 8 (2018) 4762.
[26] T.P. Joshi, G. Zhang, H. Cheng, et al., Water Res. 116 (2017) 126–134.
[27] W. Wang, Z. Zhu, M. Zhang, Q. Zhou, F. Liu, J. Taiwan, Inst. Chem. Eng. 106 (2020) 130–137.
[28] C.D. Pemmaraju, R. Copping, S. Wang, et al., Inorg. Chem. 53 (2014) 11415–11425.
[29] S. Shi, J. Yang, S. Liang, et al., Sci. Total Environ. 628-629 (2018) 499–508.
[30] B. Li, F. Liu, J. Wang, et al., Chem. Eng. J. 195 (2012) 31–39.
[31] H.A.O. Hill, P.J. Sadler, J. Biol. Inorg. Chem. 21 (2016) 5–12.